Quest Journals
Journal of Research in Environmental and Earth Sciences
Volume 10 ~ Issue 9 (2024) pp: 12-26
ISSN(Online) :2348-2532
www.questjournals.org

Research Paper

GIS based Soil Erosion Susceptibility Mapping in Middle Himalayas using MCDM: A Case Study of Rajouri District.

Mohd Mohsin Raza[1] and Yogendra Singh[2]
Department of Geology Choudhary Charan Singh University, Meerut (UP)[1,2]
[1]Corresponding author

Abstract: *The Pirpanjal range, nestled within the Himalayan region, confronts substantial soil erosion challenges owing to its diverse topography and the inherent instability of geological formations. This study focuses on the Rajouri region, to assess soil erosion susceptibility and spatially prioritize vulnerable zones. Utilizing a Geographical Information System (GIS)-based approach, we employed the Analytic Hierarchy Process (AHP) and the Weighted Sum Method (WSM). Various datasets, including precipitation records, geological maps, soil maps, and satellite imagery, were incorporated to derive eleven critical factors. These factors encompassed topographical derivatives; land use and land cover (LULC), soil properties, drainage patterns, rainfall data, lithological characteristics, wetness index, and the vegetative health of the area. The methodology employed yielded unbiased and reliable ratings and weightages, as substantiated by a Consistency Ratio (CR) of 0.095. The results reveal that 41% of the total area in the study region is exceedingly vulnerable to soil erosion. Slope variations range from 0 to 67.14 degrees, delineating high and very high susceptibility zones spanning 531.79 km² (19.82%) and 316.20 km² (11.78%) of the area, respectively. Additionally, assessments based on the Normalized Difference Vegetation Index (NDVI) and Normalized Difference Water Index (NDWI) underscore the severity of soil erosion, covering 40% and 25% of the highly susceptible zones, respectively. High drainage density and curvature zones were identified in 13% and 31% of the study area, respectively. This comprehensive study contributes valuable insights for the planning and implementation of effective soil conservation measures in the Rajouri region.*

Keywords: ***Analytical Hierarchy Process (AHP); multi criteria decision making (MCDM); pair wise comparison matrix; soil erosion susceptibility; weighted sum method***

Received 02 Sep., 2024; Revised 09 Sep., 2024; Accepted 11 Sep., 2024

Published with open access at ***www.questjournas.org***

I. Introduction

Soil erosion is undeniably a critical global issue with far-reaching ecological, economic, and social consequences. It is the process by which the topsoil, rich in essential nutrients and organic matter, is eroded and carried away by wind, water, or human activities. Soil erosion contributes to the loss of fertile topsoil, leading to decreased soil productivity (Montgomery, 2007). The loss of topsoil reduces the soil's ability to retain water, exacerbating the effects of drought (Lal, 2001). It can lead to increased use of fertilizers and pesticides to compensate for nutrient loss (Lal, 2003).The eroded sediment can clog waterways and disrupt aquatic ecosystems (Gyssels et al., 2005). - It can also result in increased sedimentation in rivers and reservoirs, impacting water quality (Hudson, 1993). Soil erosion affects approximately 24% of the world's land area, with rates varying by region (Oldeman et al., 1991). Developing countries often bear a disproportionate burden, with severe erosion problems in parts of Africa, Asia, and South America (Pimentel et al., 1995). Asia witnesses a notably high erosion rate, estimated at around 74 tons per acre annually.(El-Swaify.,1997) The rugged landscape of the Himalayas is highly prone to significant soil erosion (Singh et al.,1992), and on its own, it is responsible for 25% of the global sediment deposition into the oceans (Raymo & Ruddiman.,1992) The Himalayas experience an annual peak in ephemeral stream and river activity, combined with sufficient precipitation, leading to the effortless detachment of soil, which ultimately gives rise to a highly fragmented landscape (saini et al.,2015) Rajouri town predominantly consists of a segment of the Pir Panjal Range, which

extends in a northwest to southeast direction, exhibiting an average elevation of 9,000 feet (2,750 meters) within the middle Himalayas particularly Thanamandi and Darhal tehsils encompassing the northern regions. The ongoing uplift processes continue to cause folding, thrusting, faulting, jointing, fissuring, and shearing in this region Moreover, the seismic conditions, in addition to the long-term impacts of rivers and glaciers, have rendered the area susceptible to various forms of land degradation, including rock falls, rockslides, mudslides, debris fans, and landslides. Numerous tools have been developed by researchers to assess soil erosion, including the Soil and Water Assessment Tool (SWAT), the Water Erosion Prediction Project (WEPP), the Universal Soil Loss Equation (USLE), and the Revised Universal Soil Loss Equation (RUSLE), among others. Notably, the USLE is a widely adopted method for studying water-induced soil erosion due to its simplicity, despite the inconvenience of requiring extensive input data (Lufafa et al., 2003; Parveen and Kumar, 2012; Tiwari et al., 2000). The adaptation of the USLE leads to the Modified Universal Soil Loss Equation (MUSLE), as introduced by Williams (Williams., 1975). Subsequently, Renard (Renard.,1997) presented the Revised Universal Soil Loss Equation (RUSLE).

Diverse methodologies are employed to assess erosion risks within specific environmental contexts. One commonly used approach involves multi-criteria evaluation, which ranks and prioritizes factors based on various environmental conditions. The integration of remote sensing (RS), digital terrain modeling (DTM), and geographical information systems (GIS) has significantly enhanced our understanding of geographical patterns related to soil deterioration (Eltner et.al.,2013;Bosco et.al.,2015; Polidori & Hage.,2020). Furthermore, these technological advancements have facilitated the implementation of sustainable land and soil conservation practices (Borrelli et.al.,2016).Soil loss hazard maps play a pivotal role in understanding the extent and severity of soil loss. These maps provide critical insights that aid in making strategic policy decisions (Prasuhn et.al.,2013).Various techniques are utilized for mapping soil erosion susceptibility. The Analytic Hierarchy Process (AHP) stands out as one of the most widely adopted methods. AHP is a systematic decision-making procedure that helps prioritize areas for soil conservation measures and sustainable land management (Mushtaq et.al.,2023; Chen et.al.,2021; Pradeep.,2015).Additional techniques for mapping soil erosion include the Frequency Ratio (FR), Weights-of-Evidence (WoE), Logistic Regression (LR), and Artificial Neural Networks (ANN) (Oh.,2011). While ANN has been applied in GIS environments for soil erosion studies, it should be noted that this method often requires substantial data, which can be limiting, particularly when test data fall outside the range of training data (Kim.,2006; Lee & Pradhan.,2007).In a specific application, the Fuzzy Relations technique has been employed to map soil erosion susceptibility in Taebaek city, part of the Samcheok Coalfield in Korea (Choi et.al.,2010). However, it's important to acknowledge that the fuzzy operator method has been criticized for its lack of systematic and effective design (Ghafari & Alasty.,2004).

Various advanced methods, including the Evidential Belief Function (EBF), Weights-of-Evidence (WoE), and Adaptive Neuro-Fuzzy Inference System, have found application and testing in the fields of flooding and landslides. However, surprisingly, these methods have not been explored in soil erosion modeling (Tehrany et.al.,2017).Over time, the field of modeling has witnessed significant advancements through the integration of artificial intelligence techniques. Nonetheless, the progress in soil erosion modeling remains hampered due to the scarcity of soil erosion data and essential watershed information. A limited number of indicators and an absence of assessment methods represent significant challenges in the utilization of empirical soil erosion models. To address these limitations, a novel approach has emerged, one that seamlessly integrates empirical and artificial intelligence modeling procedures such as Kriging interpolation which can predict the values of data of the area of which data is not available. This approach has notably improved the identification of soil erosion hotspots, particularly in watersheds where soil erosion data is lacking. More recently, hybrid and ensemble models have been developed through the integration of individual machine learning (ML) models and statistical approaches. These hybrid models have gained attention for their remarkable accuracy when compared to individual models. Several publications have discussed the potential and advantages of these hybrid models, highlighting their superior performance (Kadavi et.al.,2018; Lee & Pradhan.,2006; Costache et.al.,2020).The Pirpanjal range and the adjoining areas are highly prone to soil erosion, primarily due to its diverse topography. A significant portion of its land is exposed to various forms of soil erosion, largely attributed to weak and unstable geological formations. The combined impact of these factors renders the region susceptible to erosion, leading to the depletion of soil fertility, decreased productivity, and the deterioration of water bodies. To address these challenges effectively, it is imperative to gain a comprehensive understanding of soil erosion susceptibility patterns. This understanding can guide the development of improved erosion management practices, enhanced land use policies, and efficient natural resource management for the rehabilitation of degraded land.

Given the limited existing research in the study area, our investigation has centered on various factors influencing the soil erosion process within the catchment area. This region has not been thoroughly understood and warrants closer attention and study.

II. Study Area

The study area a town in Jammu and Kashmir, India, is situated at latitude of 33.371288 and a longitude of 74.315506. It falls within the Towns category in India, pinpointed at Gps coordinates 33° 22' 16.6368" N and 74° 18' 55.8216" E. (Figure 1) The town is located within a deep valley on the southern side of the Pir Panjal Range, adjacent to the Manawar Tawi River, known as Rajouri Tawi and Naushera Tawi, flows as a tributary into the Chenab River. The study area has a span of 2682 square kilometers and boasts unique geographical characteristics. Positioned 154 kilometers away from the winter capital of Jammu, Rajouri is nestled in the foothills of the Pir Panjal Range. To its east, the district is bordered by Udhampur and Jammu, while the Line of Actual Control demarcates its southern boundary. On the west, Rajouri shares its border with Poonch district, and to the north, it neighbors Pulwama district.The region's climate is diverse, ranging from a semi-tropical climate in the southern part, encompassing areas like Nowshera, Sunderbani, and Kalakote, to a temperate climate in the mountainous northern part, including the regions of Rajouri, Thanamandi, and Koteranka tehsils within the district. The average recorded rainfall stands at approximately 500mm, while the average temperature fluctuates between 7.42 degrees Celsius and 37.4 degrees Celsius.

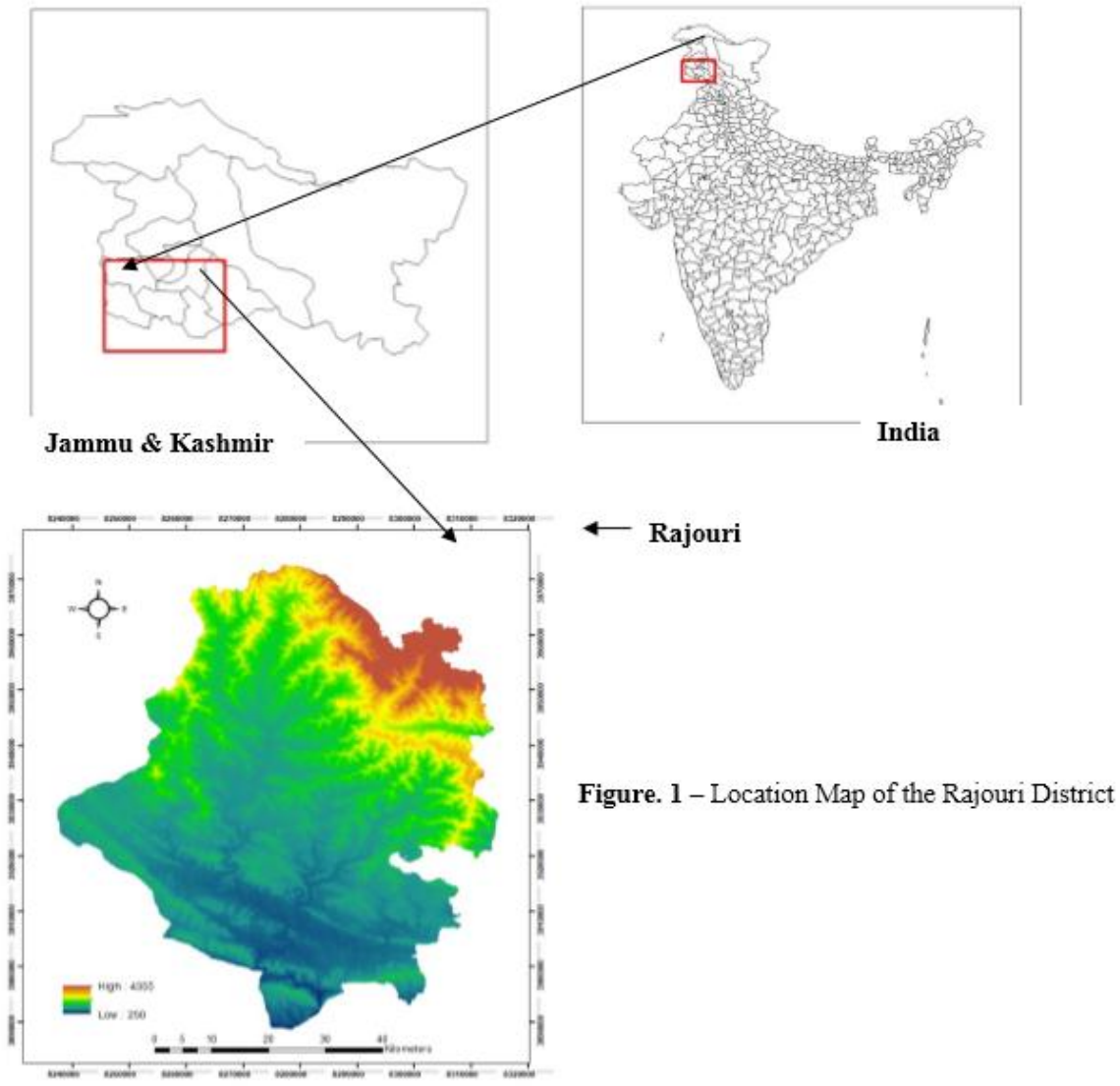

Figure. 1 – Location Map of the Rajouri District

III. Materials and Methods

In the pursuit of soil erosion susceptibility modeling, it is imperative to comprehensively prepare and assess the influence of various factors on erosion (Mosavi rt.al.,2020). This study leveraged a diverse array of data types and sources, including satellite data, digital elevation models, geological data, soil data, and meteorological data.The foundational datasets utilized in this study encompassed:- Base map of india ,Digital

Elevation Model (DEM) at a resolution of 30 meters..Satellite imagery from Cartosat 1B with a remarkable resolution of 2.5 meters...Indian Remote Sensing (IRS) data captured via Linear Imaging Self Scanning (LISS)-III with a resolution of 23.5 meters...Landsat 8 Operational Land Imager (OLI) imagery at a resolution of 30 meters.Daily rainfall data from the Indian Meteorological Department (IMD) spanning from 1980 to 2022 and lithology data from survey of india at a 1:50000 scale.To access the required data, the following sources and portals were used:-Cartosat DEM from (https://bhuvan-app3.nrsc.gov.in/) .Landsat 8 OLI satellite imagery were acquired from the USGS Earth Explorer data portal (https://earthexplorer.usgs.gov/) .Cartosat 1B and IRS-LISS III satellite imagery were procured from the National Remote Sensing Center, ISRO's EO data hub (https://bhoonidhi.nrsc.gov.in) .Rainfall data was obtained from the Indian Meteorological Department (https://mausam.imd.gov.in/). Base map of india shapefile (http://www.indiaremotesensing.com/). Remote Sensing Data Utilization Cartosat 1B and IRS-LISS III satellite imagery played a pivotal role in the preparation of land use/land cover, lithology, and soil layers. Meanwhile, the SRTM DEM data facilitated the derivation of topographical parameters and drainage analysis for the study area. Additionally, Landsat-8 OLI satellite imagery was harnessed for the generation of water and vegetation indices, and rainfall data contributed to the calculation of the rainfall erosivity factor. To ensure uniformity and compatibility, all datasets were projected into a common projection system, specifically Universal Transverse Mercator (UTM). Resampling was performed using the nearest neighbor technique. Detailed methodology employed in soil erosion susceptibility modeling refers to Figure 2.

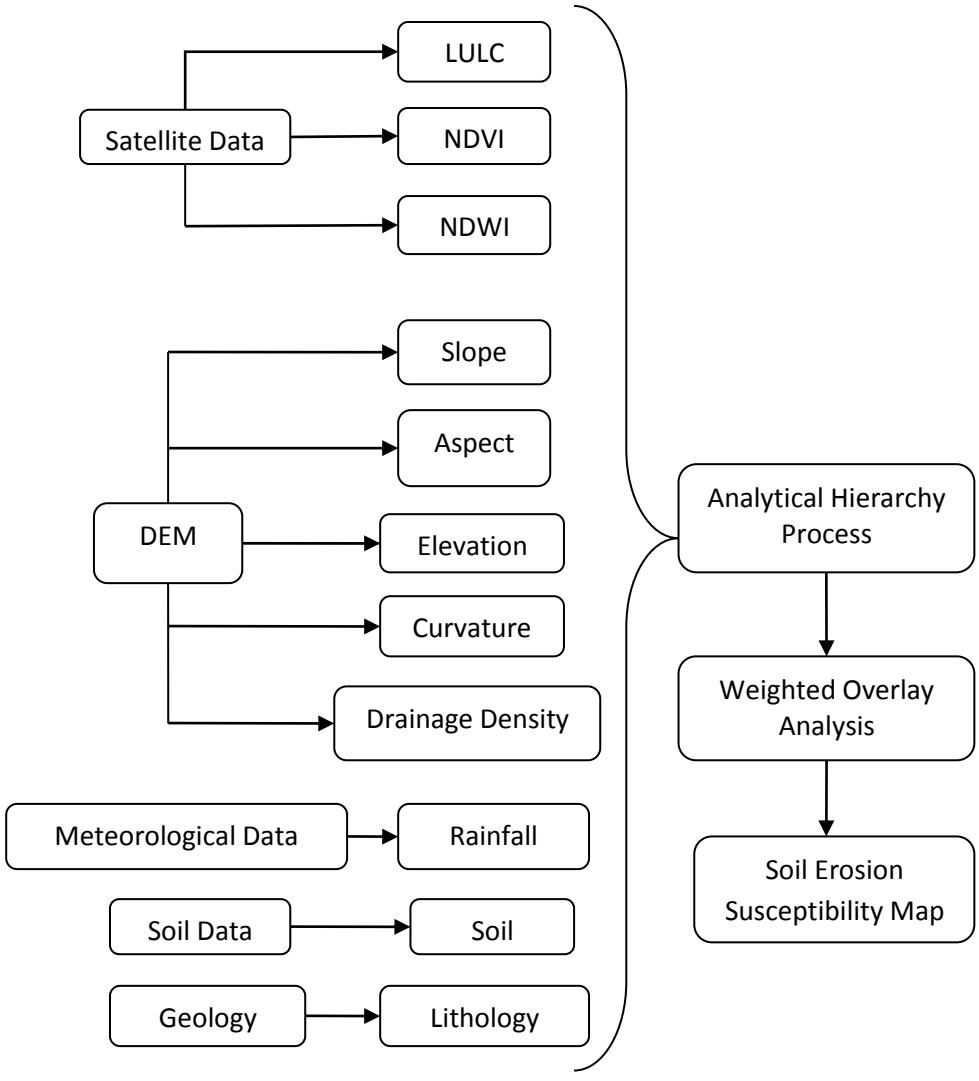

Figure. 2 – Detailed Methodology

3.1.Soil Erosion Parameters

In the study area catchments analysis, the selection of eleven influencing factors (elevation, slope, aspect, curvature, soil, land use/cover, drainage density, rainfall erosivity, lithology, NDWI, and NDVI) was based on a combination of regional understanding, area-specific experience, and a comprehensive review of the existing literature (Aslam et.al.,2021; Conoscenti et.al.,2008; Halefom & Teshome.,2019) The rationale behind the choice of each of these eleven parameters and the methods used to generate them are explained below:

Aspect (A_S): Determining the direction of slope, known as aspect, is a critical factor in erosion dynamics. For instance, north-facing slopes generally exhibit lower erosion risks compared to south-facing slopes. We categorized slope direction into nine classes, including flat, north, northeast, east, southeast, south, west, southwest, and northwest (Figure 3a).

Slope (S_L): The runoff velocity and infiltration rate are closely linked to the slope angle. Steeper slopes tend to have higher runoff velocities, which can lead to increased erosion rates compared to gentle slopes where the infiltration rate is higher. To assess the impact of slope gradient on erosion, we generated a slope map in degrees using ArcGIS, utilizing DEM data for our study area (Figure 3b).

Curvature *(C_U)*: Curvature quantifies the extent to which a surface deviates from a straight path, influencing the convergence and divergence of water flow with respect to the slope. We derived this layer from DEM data using proximity analysis (Figure 3c)

Elevation(E_L): Elevation is a key factor influencing erosion rates due to its impact on several components, including soil moisture, water balance, erosional and depositional processes, soil organic matter, biomass, and the production of cultivated plants and natural flora (Halefom & Teshome.,2019). We obtained the elevation layer from SRTM DEM data and processed it to classify it, preparing it for use as input in our overlay analysis (Figure 3d).

Rainfall Erosivity Factor (R_E): Rainfall erosivity is a key factor in triggering soil loss from hill slopes. It depends on precipitation characteristics such as volume, magnitude, and seasonal distribution. Due to limited access to high-resolution precipitation databases for the area, we employed empirical models to estimate rainfall erosivity. We used the relationship developed by (Singh., 1981) .evaluate the rainfall erosivity factor (Figure 3e).

Land Use/Land Cover (L_{ULC}): LULC is a crucial factor in various hydrological processes, including infiltration, runoff velocity, evapotranspiration, and soil erosion. We derived the LULC map from Cartosat-1B data (2.5m resolution) through on-screen digitization and selective ground truthing. (Figure 3f).

Soil (S_O): Soil type plays a significant role in susceptibility to soil erosion and is influenced by characteristics such as texture, organic matter content, parent material, porosity, structure, and infiltration potential. We created the soil layer after conducting selective ground truthing, using the soil texture map from the Indian Soil and Land Use Survey, (Figure 3g).

Drainage Density (D_D): The drainage network is a significant variable affecting erosion in mountainous areas. It erodes sediment deposits, transporting them to water bodies. Areas with dense drainage networks have a higher probability of soil erosion. We delineated the drainage network from the DEM (Figure 3h).

Normalized Difference vegetation Index (N_{DVI}): quantifies vegetation health by comparing the reflection of near-infrared and red light. Healthy vegetation reflects more near-infrared and absorbs more red light, resulting in a higher NDVI value, usually ranging from -1 to +1.In our analysis, NDVI is calculated using satellite data (Figure 3i). It helps assess vegetation density, land cover types, crop health, environmental changes, drought conditions, carbon sequestration, and wildlife habitats. NDVI is a versatile tool in environmental monitoring and land management.

Normalized Difference Water Index (N_{DWI}): NDWI represents the water content of vegetation and is defined as the ratio of water flow erosion intensity, assuming the flow rate is sufficient for a specific area. It is often influenced by regional climate and soil characteristics that control water availability. The index is calculated from the ratios of the green and NIR bands of OLI satellite data (Figure 3j).

Lithology (L_I): Lithological conditions are important for controlling erosional processes, affecting the nature of alluvial features, slopes, soil types, raw materials, and sediments.

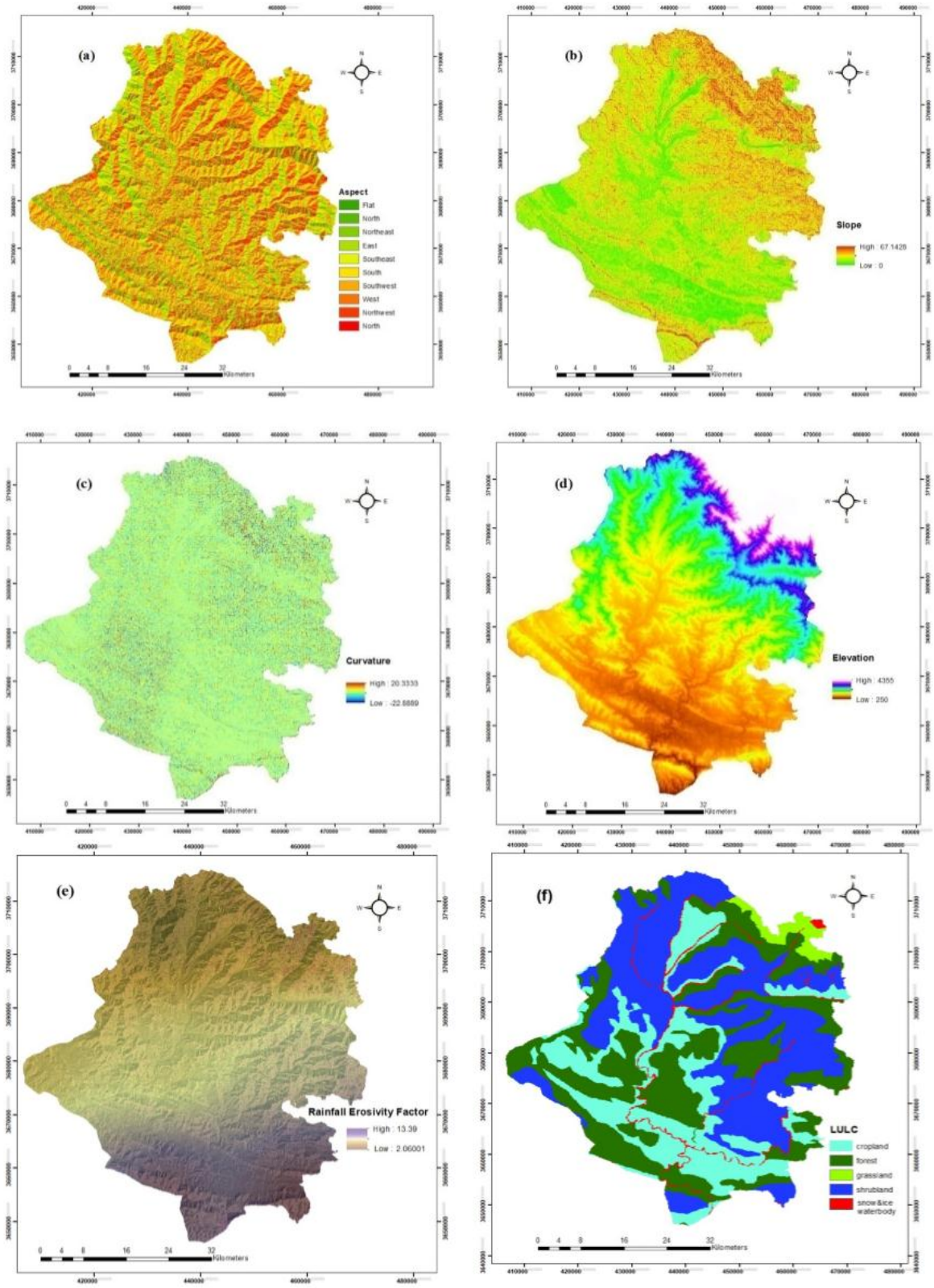
(a)
Aspect
Flat
North
Northeast
East
Southeast
South
Southwest
West
Northwest
North
(b)
Slope
High : 67.1428
Low : 0
(c)
Curvature
High : 20.3333
Low : -22.8889
(d)
Elevation
High : 4355
Low : 250
(e)
Rainfall Erosivity Factor
High : 13.39
Low : 2.06001
(f)
LULC
cropland
forest
grassland
shrubland
snow&ice
waterbody
Kilometers

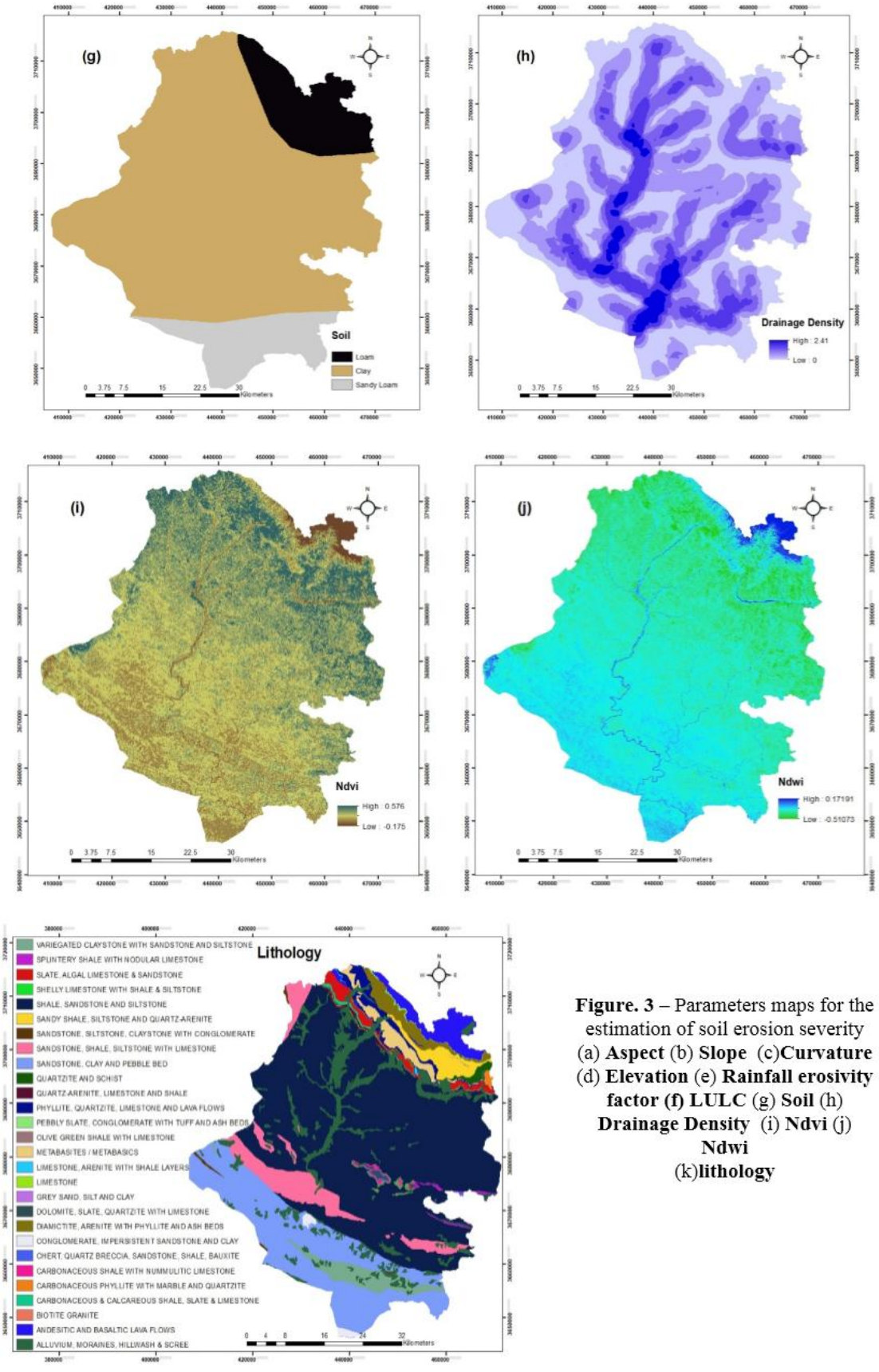

Figure. 3 – Parameters maps for the estimation of soil erosion severity (a) **Aspect** (b) **Slope** (c)**Curvature** (d) **Elevation** (e) **Rainfall erosivity factor (f) LULC** (g) **Soil** (h) **Drainage Density** (i) **Ndvi** (j) **Ndwi** (k)**lithology**

3.2. Determination of Weights by the AHP Procedure

The Analytic Hierarchy Process (AHP), also referred to as the Saaty method, is a versatile semi-quantitative technique widely utilized in modeling soil erosion risk (Aslam et al.,2021;Pradeep et.al.,2015; Wu&Wang.,2007).AHP employs a structured methodology, systematically decomposing intricate decisions into a hierarchical framework comprising distinct levels for criteria and alternatives (Senouci et al., 2021). In our study, AHP is applied to prioritize parameters influencing soil erosion and to construct a Soil Erosion susceptibility map for the Rajouri District.

Hierarchy Construction: In the AHP method, the initial step involves creating a hierarchical structure to systematically break down the decision problem into manageable components (Saaty, 1980). This hierarchy typically comprises three main levels: Goal, Criteria, and Alternatives. At the highest level, the primary goal is defined, which in this case, is the development of a landslide susceptibility map for the Pirpanjal Range. The second level includes criteria that have a significant impact on landslide occurrence, including factors such as slope angle, geology/lithology, land cover, precipitation, distances from roads, streams, faults, topographic wetness index (TWI), aspect, curvature, and relative relief. The lowest level contains the available alternatives, representing different values or states for each criterion.

Pairwise Comparisons:Pairwise comparisons are a pivotal component of the AHP method, enabling experts and stakeholders to express their preferences between criteria and alternatives (Saaty, 1980). A scale ranging from 1 to 9 is utilized to indicate the relative importance of elements, with 1 denoting equal
importance and 9 indicating extreme importance. These pair wise comparisons result in the generation of a matrix, known as the pair wise comparison matrix, which quantifies the relationships between the various elements.(Table.1)

Ordinal Scales	Degree of Preference
1	Equally important
3	Moderately important one over the other
5	Strongly important one over the other
7	Very strongly important one over the other
9	Extremely important one over the other
2,4,6,8	Intermediate values

Table.1- Pairwise comparison Saaty's method(Saaty, 1980).

Calculation of Priority Weights:The data obtained from the pair wise comparisons is used to calculate the priority weights of criteria and alternatives (Saaty, 1980). The Eigenvalue method or Eigenvector method, based on the largest Eigenvalue principle, is commonly employed for this purpose. The priority weights represent the relative significance of each criterion and alternative in contributing to the overall goal of landslide susceptibility mapping.

Consistency Analysis:To ensure the reliability of the decision-making process, it is essential to assess the consistency of judgments made during pair wise comparisons (Saaty, 1980). Saaty (1980) introduced the Consistency Ratio (CR) as a measure of consistency. A CR value greater than 0.1 indicates some level of inconsistency in the judgments, raising the need for reevaluation and adjustment.

$$\mathbf{CI = (\lambda\text{-}n)/(n\text{-}1)}$$

Where λ is the max value of eigenvector and n is the number of criteria.

Saaty (2000) generated a reciprocal matrix randomly by using scales ranging from 1/9 to 9. The purpose was to obtain a random consistency index (RI) and assess if it falls within the range of approximately 10% (0.1) or below. Additionally, Saaty (1977) introduced the consistency ratio (CR), depicted in equation 2, which involves comparing the consistency index with the random consistency index to evaluate their similarities.

$$\mathbf{CR=CI/RI}$$

Where RI is the Random Index, and CI stands for Consistency Index.

Number	1	2	3	4	5	6	7	8	9	10	11	12	13	14	15
Random Index	0	0	0.58	0.9	1.12	1.24	1.32	1.41	1.45	1.49	1.51	1.53	1.56	1.57	1.59

Table.2- Random consistency index (RI) (Saaty, 1980)

3.3.Weighted Sum Method (WSM)

To implement the Weighted Sum Model (WSM), all the selected factors were reclassified into five priority classes: very low, low, medium, high, and very high (Table 3). These class ranges were derived from each raster layer after reclassification. The natural break classification method was employed in ArcGIS to optimize the grouping of values into "natural" classes. The assignment of five priority classes was based on existing literature (Mushtaq & Lala.,2017; Pandey et.al.,2009; Amin & Romshoo, 2019) Within each layer, a

rating from very low (1) to very high (5) was assigned to the classes in increasing order of their qualitative importance for erosion. The rankings were determined for each parameter, and their respective classes depended on the functional relationship with soil erosion severity. Higher scale values were assigned to cells highly prone to soil erosion, while lower values were given to cells less prone to erosion.

Subsequently, soil erosion severity was assessed on a pixel basis using the Weighted Sum Model (WSM). In the WSM, each parameter under consideration was multiplied by its respective weight, and the sum of all the layers resulted in a soil severity index.

S.No	Layers	Classes	Scale	Soil Severity
1.	**Slope (degree)**	0°-9.74°	1	Very low
		9.74°-17.90°	2	low
		17.90° - 25.80°	3	Medium
		25.80° - 34.75°	4	High
		34.75° - 67.14°	5	Very high
2.	**Aspect**	0 – 69.7	1	Very low
		69.7 – 144.7	2	low
		144.7 – 215.4	3	Medium
		215.4 – 286.2	4	High
		286.2 – 359.8	5	Very high
3.	**Lithology**	• Andesitic and basaltic lava flows • Biotite granite • Carbonaceous phyllite with marble and quartzite • Chert, quartz breccia, sandstone, shale, bauxite • Dolomite, slate, quartzite with limestone • Metabasites / metabasics • Phyllite, quartzite, limestone and lava flows • Quartzite and schist • Slate, algal limestone & sandstone	1	Very low
		• Conglomerate, impersistent sandstone and clay • Diamictite, arenite with phyllite and ash beds • Limestone • Limestone, arenite with shale layers • Sandy shale, siltstone and quartz-arenite • Splintery shale with nodular limestone	2	low
		• Carbonaceous,calcareous shale, slate, limestone • Olive green shale with limestone • Quartz-arenite, limestone and shale • Sandstone, clay and pebble bed • Sandstone, shale, siltstone with limestone • Sandstone, siltstone, claystone, conglomerate • Shale, sandstone and siltstone • Variegated claystone sandstone and siltstone	3	Medium
		• Carbonaceous shale with nummulitic limestone • Pebbly slate,conglomerate with tuff and ash bed	4	High
		• Alluvium, moraines, hillwash & scree • Grey sand, silt and clay • Shelly limestone with shale & siltstone	5	Very high
4.	**Soil**	Clay	1	Very low
		Sandy Loam	2	low
		Loam	3	Medium
5.	**LULC**	Snow&ice, waterbody	1	Very low
		Forest	2	low
		Shrubland	3	Medium
		Cropland	4	High
		Grassland	5	Very high
6.	**Ndwi**	-0.51 – -0.31	1	Very low
		-0.31 - -0.26	2	low
		-0.26 - -0.21	3	Medium
		-0.21 - -0.12	4	High
		-0.12 – 0.17	5	Very high
7.	**Ndvi**	-0.17 – 0.11	1	Very low
		0.11 – 0.22	2	low
		0.22 – 0.27	3	Medium
		0.27 – 0.34	4	High
		0.34 – 0.57	5	Very high
8.	Rainfall	2.06 – 4.77	1	Very low
		4.77 – 6.76	2	low
		6.76 – 8.41	3	Medium

		8.41 – 10.41 10.41 -13.38	4 5	High Very high
9.	**Drainage Density**	0 – 0.321 0.321–0.612 0.612–0.893 0.893–1.384 1.384–2.41	1 2 3 4 5	Very low low Medium High Very high
10.	**Curvature**	-22.8 - -2.54 -2.54 - -0.85 -0.85 - 0.50 0.50 – 2.19 2.19 – 20.3	1 2 3 4 5	Very low low Medium High Very high
11.	**Elevation**	250-843 843-1271 1271-1858 1858 -2725 2725-4355	1 2 3 4 5	Very low low Medium High Very high

Table.3- Scale value assigned to different thematic layers for soil erosion severity.

IV. Results and Discussions

As described in the Methods section, the Pairwise Comparison Matrix (PCM) was utilized to determine the criteria weights for each parameter following the Analytic Hierarchy Process (AHP) methodology. The rankings were established based on both local knowledge of the study area and insights from relevant literature (Pradeep et.al.,2015;Mushtaq&lala.,2017;Pandey et.al.,2009;Ashraf.,2020).The ratings and weightages employed in this study were found to be unbiased and reliable, as demonstrated by the calculated consistency ratio (CR) of 0.095 in the PCM (Table 4).

This CR value aligns with the results obtained by (Das et.al.,2020). (Jaiswal et al.,2014) similarly found a consistency ratio of 0.093 or 9.3% to be acceptable, suggesting that when CR is below 10%, inconsistencies in decision-making are tolerable, and the derived weights can be confidently utilized for priority assessment.The calculation of soil erosion severity at the pixel level was determined by employing Equation, as provided below.

$$SES = E_{Lw} \times 0.245 + S_{Lw} \times 0.180 + A_{Sw} \times 0.131 + C_{Uw} \times 0.110 + S_{Ow} \times 0.086 + L_{ULCw} \times 0.069 + D_{Dw} \times 0.052 + R_{Ew} \times 0.039 + L_{Iw} \times 0.031 + N_{DWIw} \times 0.028 + N_{DVIw} \times 0.024$$

Where SES shows the areas of soil erosion severity.E_L,S_L,A_S,C_U,S_O,L_{Ulc},D_D,R_E,L_I, N_{DWI},andN_{DVI} represent the layers of elevation, slope, aspect, curvature, soil, LULC, drainage density, rainfall erosivity,lithology,NDVI,andNDWI.The weight of a layer and of a particular parameter is represented by *w*.

Factors	E_L	S_L	A_S	C_U	S_O	L_{ULC}	D_D	R_E	L_I	N_{DWI}	N_{DVI}	Normalied Weights
E_L	1	1	3	3	7	5	5	7	7	9	5	0.2457
S_L	1	1	3	2	3	4	5	5	4	3	3	0.1801
A_S	1/3	1/3	1	3	2	3	4	5	5	4	3	0.1317
C_U	1/3	1/2	1/3	1	3	2	3	4	5	5	4	0.1106
S_O	1/7	1/3	1/2	1/3	1	3	2	3	4	5	5	0.0865
L_{ULC}	1/5	1/4	1/3	1/2	1/3	1	3	2	3	4	5	0.0693
D_D	1/5	1/5	1/4	1/3	1/2	1/3	1	3	2	3	4	0.0521
R_E	1/7	1/5	1/5	1/4	1/3	1/2	1/3	1	3	2	3	0.0390
L_I	1/7	1/4	1/5	1/5	1/4	1/3	1/2	1/3	1	3	2	0.0318
N_{DWI}	1/9	1/3	1/4	1/5	1/5	1/4	1/3	1/2	1/3	1	3	0.0284
N_{DVI}	1/5	1/3	1/3	1/4	1/5	1/5	1/4	1/3	1/2	1/3	1	0.0248

Table.4 Pairwise comparison matrix.

4.1.Soil Erosion Susceptibility Classes

The final map of soil erosion susceptibility for Rajouri District, prepared using a GIS-based approach, is presented in (Figure 4). The derived layer was categorized into five classes based on natural break classification: very low, low, medium, high, and very high (Table 5).

In total, 31.6% (847.99 km^2) of the region was identified as highly susceptible to erosion, encompassing high and very high susceptibility zones. These areas are primarily situated at very high elevations and mostly consist of wasteland. The presence of steep slopes and more erodible soil particles in these regions contributes to their higher susceptibility to soil loss. The undulating topography, steep slopes, and heavy rainfall in the Himalayan region predispose it to natural hazards, including soil erosion (Chalise et.al.,2018).

The medium susceptible class covered an area of 25.39% (681.46 km^2), primarily associated with forest cover. Forested areas offer effective protection against surface runoff and soil erosion losses (McDonald et al.,2002). Despite this, they are categorized as moderate susceptibility areas because most forested land is situated on steep slopes and at higher elevations compared to agricultural and built-up areas, which are on relatively less

steep slopes and at lower elevations. This difference in elevation and slope steepness may explain the comparatively higher soil erosion severity in forested land use compared to other land uses.

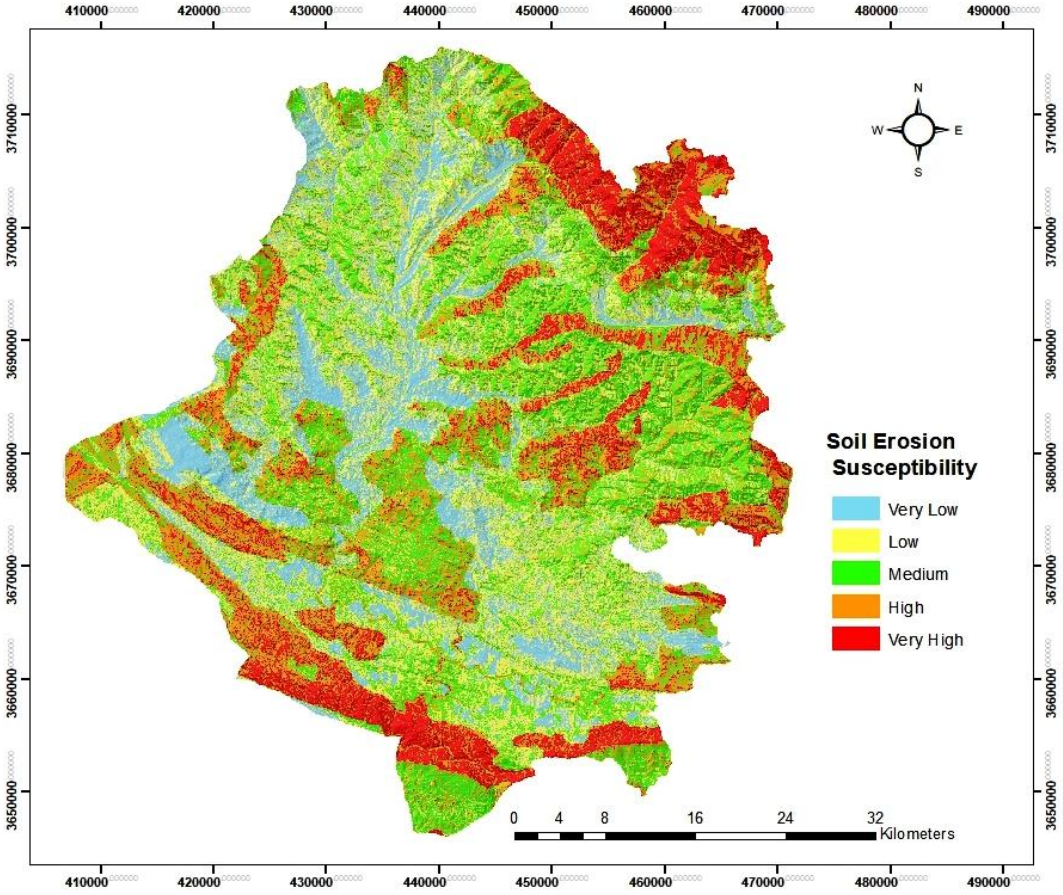

Figure. 4 Soil erosion severity map of Rajouri District

It was observed that 42.98% (1153.52 km^2) of the area fell under the categories of very low to low soil erosion severity. These areas are predominantly located at lower elevations, mainly consisting of valley floors where agriculture and built-up land use are dominant.

Very Low		Low		Medium		High		Very High	
Area (km^2)	(%)	Area (km^2)	(%)	Area (km^2)	(%)	Area (km^2)	(%)	Area (km^2)	(%)
424.42	15.81%	729.10	27.17%	681.46	25.39%	531.79	19.82%	316.20	11.78%

Table.5 susceptibility classes of erosion

Soil Erosion SusceptibilityClass	E_L		S_L		A_S		C_U		S_O		L_{ULC}	
	Km^2	%	Km^2	%	Km^2	%	Km^2	%	Km^2	%	Km^2	%
Very Low	1427	53%	607	23%	477	17%	167	6%	2099	77%	57	2%
Low	999	37%	874	32%	500	19%	595	22%	280	11%	902	34%
Medium	196	7%	776	29%	654	25%	1087	41%	304	12%	1026	38%
High	59	2.93%	349	13%	601	23%	642	24%	-	-	638	24%
Very High	2	0.07%	76	3%	452	17%	191	7%	-	-	60	2%
Total	2683											

Table.6 Percentage distribution of elevation,slope,aspect,curvature,soil,and lulc

Soil Erosion SusceptibilityClass	*DD*		*REF*		*LITH*		*NDWI*		*NDVI*	
	Km²	%	Km²	%	Km²	%	Km²	%	Km²	%
Very Low	1005	38%	445	17%	230	9%	296	11%	53	2%
Low	773	28%	469	18%	127	5%	705	26%	492	18%
Medium	559	21%	845	31%	2052	76%	1007	38%	1079	40%
High	262	10%	431	16%	9	0.33%	612	23%	763	29%
Very High	83	3%	492	18%	266	9.67%	62	2%	295	11%
Total	2683									

Table.7 Percentage distribution of drainage density,rainfall factor, lithology,Ndwi and Ndvi

4.2.Soil Erosion Influencing Parameters

The quantitative and qualitative results of the vulnerability of soil erosion, obtained through zonal statistics, are presented in Tables 6 and 7.

Elevation plays a significant role in shaping soil erosion patterns within mountainous regions (Aslam et.al.,2021). It influences factors such as plant distribution, physiography, and morphology (Chapin et.al.,1987). In our study area, elevation ranged from 250 to 4355 meters.

Among the total conservation area in 2023, approximately 53% of the land fell within an elevation range of 250–843 meters. Elevation ranges of 843–1858 meters and 1858–4355 meters covered approximately 44% and 4% of the study area, respectively.

Slope gradient is another critical factor influencing soil erosion, particularly with regard to steepness (Kachouri et.al.,2015). The slopes in our study area varied from 0 to 67.14 degrees, with the largest portion, approximately 32%, falling within the 9.74–17.90 degree range, followed by 29% within the 17.90–25.80 degree range. 16% (425 square kilometers) of the area was highly susceptible to erosion, 29% (776 square kilometers) fell into the medium category, and 55% (1481 square kilometers) were distributed among the very low to low susceptibility zones. The higher slope values can be attributed to abrupt variations near drainage channels and highly dissected topography, which makes these areas more vulnerable to soil erosion due to increased runoff velocity and associated material transport (Singh.,1981).

Aspect, the compass direction a slope faces, also plays a critical role in influencing vegetation patterns and erosion (Yang.,2020). Aspect interacts with other environmental variables such as slope position, jointly influencing vegetation structure (Méndez-Toribio.,2016). In our study area, approximately 40% (1053 square kilometers) of the land was highly susceptible to erosion, primarily in the aspect range of 215.4–359.8 degrees. The least and moderately susceptible zones covered 977 square kilometers and 654 square kilometers, respectively.

The curvature of the hillslope significantly influences stream density and watershed morphology, further impacting soil erosion (Halefom,&Teshome.,2019). Curvature distribution in our study area revealed that the medium curvature zone covered the largest portion, approximately 41% (1087 square kilometers), followed by the low zone at 28% (762 square kilometers) and the high zone at 31% (833 square kilometers).

Drainage density, an index of soil erosion, also played a role in susceptibility, with 38% (1005 square kilometers) and 28% (773 square kilometers) of the area falling within very low to low zones, followed by 21% (559 square kilometers) in the medium class, 10% (262 square kilometers) in the high class, and 3% (83 square kilometers) in the very high class. Higher drainage density signifies a greater number of streams, leading to a higher potential for soil erosion.

Rainfall is a crucial factor that can cause soil erosion due to the impact of raindrops and runoff (Saini et.al.,2015). The rainfall erosivity index in our study area ranged from 2.06 to 13.38, Rainfall erosivity distribution indicated that 31% (845 square kilometers) of the area fell within the medium zone, followed by 18% (469 & 492 square kilometers) in the low zone and very high zone.17% (445 square kilometers) in the very low zone. Rainfall erosivity values tended to increase from the alluvial plain region in the south/southwest, which had the lowest elevation, towards the hilly areas in the northeast.

The type of land use and land cover (LULC) has a strong influence on soil erosion processes (Makaya, et.al.,2019). In our study, approximately 26% (698 square kilometers) of the LULC was highly susceptible to erosion, while 38% (1026 square kilometers) was moderately sensitive, and 36% (959 square kilometers) exhibited the least sensitivity to erosion. The higher susceptibility was largely due to the prevalence of wasteland. Moderately sensitive zones were primarily forested, followed by agricultural land .Forested areas are known for their ability to control soil erosion due to the presence of dense vegetation and extensive root biomass (Rather et.al.,2017).

Lithology, which refers to the physical properties of rocks, also influences soil erosion (Aslam et.al.,2021). In our study, the area has different lithologies and the lithologies falling in medium zones are approximately 76% covering (2052 square kilometers), followed by low zones 14% covering (457 square kilometers) and high zones 10% covering (275 square kilometers).

Normalized Difference Vegetation Index (NDVI) and Normalized Difference Water Index (NDWI) are indicators of vegetation health and wetness, respectively (Saha.,2018). Good vegetation cover with positive NDVI values can reduce erosion, while areas with higher NDWI values are more susceptible to erosion. In our study, both NDVI and NDWI reclassified maps showed similar distributions, with approximately 40% (1058 square kilometers and 25%(674 square kilometers, respectively) falling within highly susceptible erosion zones.

Soil texture also plays a role in erosion susceptibility as it affects water infiltration rates. Our results indicated that 77% (2099 square kilometers) of the area had very low erosion severity, 11% (280 square kilometers) had low erosion severity, and 12% (304 square kilometers) had medium erosion severity, largely due to the prevalence of loam soil texture in the study area.

This comprehensive analysis of various factors influencing soil erosion patterns highlights the complex interactions in mountainous regions and provides valuable insights for erosion control and land management efforts

V. Conclusion

The study utilized Geographic Information System (GIS) in combination with the Analytic Hierarchy Process (AHP) to assess the susceptibility of soil erosion in the Rajouri District region. AHP was employed to reduce biases in decision-making and effectively handle multiple criteria and complex decisions. The framework was built upon the analysis of eleven parameters derived from satellite imagery, geological data, soil information, and precipitation data. These parameters were used to categorize the severity of soil erosion into five classes: very low, low , medium, and high and very high.The results indicated that most of the selected parameters had a significant impact on soil erosion in mountainous areas. Among these, topographical features, land use/land cover (LULC), and lithology had the most pronounced effects, followed by vegetation, moisture, precipitation, and soil types. Notably, LULC and lithology accounted for 26% and 10%% of the total area under the very high susceptibility category for soil erosion. Other influential factors included aspect (40%), rainfall erosivity (18%), elevation, (3%), and slope (16%). The Normalized Difference Vegetation Index (NDVI) and Normalized Difference Water Index (NDWI) covered 40% and 25% of the total study area, respectively.

It was evident that both LULC and lithology type influenced soil erosion, but aspect played a crucial role in mountainous terrain by regulating temperature, moisture, water supply, vegetation, and soil development. One major contributing factor to soil loss in the study area was the lack of knowledge about agricultural practices on steep and high-altitude slopes. Aspect, drainagedensity, and curvature, combined with lithology, had a significant impact on soil loss vulnerability.

Regions with high precipitation and wetness indices were found to be highly erosive, particularly in areas with barren land. The applied methodology proved to be an effective and timely approach for qualitatively assessing erosion susceptibility over a large area. This approach can be valuable for planners and policymakers when implementing conservation measures. The study makes a substantial contribution to providing useful predictions for decision-makers and authorities to minimize potential damage from soil erosion in the Sind and Dachigam catchments.

To reduce soil loss, it is essential to evaluate existing scientific management practices and implement appropriate conservation measures at the catchment level. Recommended strategies include afforestation, urban tree plantation, controlling overgrazing, contour farming, water conservation systems, flood and erosion control systems, and runoff water catchment systems. The aspect factor, as a macro factor, needs consideration as it influences the overall erosion process.

Additionally, adopting conservation measures like no-till (NT) practices, which involve sowing directly into stubble without ploughing, can minimize soil disturbance. NT practices have environmental benefits, including reduced erosion risk due to improved soil structure and continuous plant cover. These measures not only help reduce soil loss but also promote soil health and crop productivity, ultimately improving the livelihoods of the local population.

However, it's important to acknowledge that uncertainties are inherent in the conditioning factors, and expert evaluations may introduce subjectivity. Hence, future assessments of soil erosion susceptibility should consider fuzzy approaches or machine learning algorithms, along with other significant factors such as spatiotemporal changes in rainfall distribution and frequency under climate change scenarios.

References

[1]. Amin, M., & Romshoo, S. A. (2019). Comparative assessment of soil erosion modelling approaches in a Himalayan watershed. Modeling Earth systems and environment, 5, 175-192.

[2]. Ashraf, A. (2020). Risk modeling of soil erosion under different land use and rainfall conditions in Soan river basin, sub-Himalayan region and mitigation options. Modeling Earth Systems and Environment, 6(1), 417-428.

[3]. Aslam, B., Maqsoom, A., Alaloul, W. S., Musarat, M. A., Jabbar, T., & Zafar, A. (2021). Soil erosion susceptibility mapping using a GIS-based multi-criteria decision approach: Case of district Chitral, Pakistan. Ain Shams Engineering Journal, 12(2), 1637-1649.

[4]. Borrelli, P., Paustian, K., Panagos, P., Jones, A., Schütt, B., & Lugato, E. (2016). Effect of good agricultural and environmental conditions on erosion and soil organic carbon balance: a national case study. Land use policy, 50, 408-421.

[5]. Bosco, C., de Rigo, D., Dewitte, O., Poesen, J., & Panagos, P. (2015). Modelling soil erosion at European scale: towards harmonization and reproducibility. Natural Hazards and Earth System Sciences, 15(2), 225-245.

[6]. Chalise, D., Kumar, L., Shriwastav, C. P., & Lamichhane, S. (2018). Spatial assessment of soil erosion in a hilly watershed of Western Nepal. Environmental Earth Sciences, 77, 1-11.

[7]. Chapin, F. S., Oechel, W. C., Van Cleve, K., & Lawrence, W. (1987). The role of mosses in the phosphorus cycling of an Alaskan black spruce forest. Oecologia, 74, 310-315.

[8]. Chen, S., Liu, W., Bai, Y., Luo, X., Li, H., & Zha, X. (2021). Evaluation of watershed soil erosion hazard using combination weight and GIS: A case study from eroded soil in Southern China. Natural Hazards, 109, 1603-1628.

[9]. Choi, J. K., Kim, K. D., Lee, S., & Won, J. S. (2010). Application of a fuzzy operator to susceptibility estimations of coal mine subsidence in Taebaek City, Korea. Environmental Earth Sciences, 59, 1009-1022.

[10]. Conoscenti, C., Di Maggio, C., & Rotigliano, E. (2008). Soil erosion susceptibility assessment and validation using a geostatistical multivariate approach: a test in Southern Sicily. Natural Hazards, 46, 287-305.

[11]. Costache, R., Ngo, P. T. T., & Bui, D. T. (2020). Novel ensembles of deep learning neural network and statistical learning for flash-flood susceptibility mapping. Water, 12(6), 1549.

[12]. Das, B., Bordoloi, R., Thungon, L. T., Paul, A., Pandey, P. K., Mishra, M., & Tripathi, O. P. (2020). An integrated approach of GIS, RUSLE and AHP to model soil erosion in West Kameng watershed, Arunachal Pradesh. Journal of Earth System Science, 129, 1-18.

[13]. El-Swaify, S. A. (1997). Factors affecting soil erosion hazards and conservation needs for tropical steeplands. Soil technology, 11(1), 3-16.

[14]. Eltner, A., Mulsow, C., & Maas, H. G. (2013). Quantitative measurement of soil erosion from TLS and UAV data. The International Archives of the Photogrammetry, Remote Sensing and Spatial Information Sciences, 40, 119-124.

[15]. Ghafari, A. S., & Alasty, A. (2004, June). Design and real-time experimental implementation of gain scheduling PID fuzzy controller for hybrid stepper motor in micro-step operation. In Proceedings of the IEEE International Conference on Mechatronics, 2004. ICM'04. (pp. 421-426). IEEE.

[16]. Gyssels, G., Poesen, J., Bochet, E., & Li, Y. (2005). Impact of plant roots on the resistance of soils to erosion by water: a review. Progress in physical geography, 29(2), 189-217.

[17]. Halefom, A., & Teshome, A. (2019). Modelling and mapping of erosion potentiality watersheds using AHP and GIS technique: a case study of Alamata Watershed, South Tigray, Ethiopia. Modeling Earth Systems and Environment, 5(3), 819-831.

[18]. Hudson, N. (1993). Field measurement of soil erosion and runoff (Vol. 68). Food & Agriculture Org..

[19]. Jaiswal, R. K., Thomas, T., Galkate, R. V., Ghosh, N. C., & Singh, S. (2014). Watershed prioritization using Saaty's AHP based decision support for soil conservation measures. Water resources management, 28, 475-494.

[20]. Kachouri, S., Achour, H., Abida, H., & Bouaziz, S. (2015). Soil erosion hazard mapping using Analytic Hierarchy Process and logistic regression: a case study of Haffouz watershed, central Tunisia. Arabian Journal of Geosciences, 8, 4257-4268.

[21]. Kadavi, P. R., Lee, C. W., & Lee, S. (2018). Application of ensemble-based machine learning models to landslide susceptibility mapping. Remote Sensing, 10(8), 1252.

[22]. Kim, K. D., Lee, S., Oh, H. J., Choi, J. K., & Won, J. S. (2006). Assessment of ground subsidence hazard near an abandoned underground coal mine using GIS. Environmental Geology, 50, 1183-1191.

[23]. Lal, R. (2003). Soil erosion and the global carbon budget. Environment international, 29(4), 437-450.

[24]. Lal, R. A. T. T. A. N. (2001). Soil degradation by erosion. Land degradation & development, 12(6), 519-539.

[25]. Lee, S., & Pradhan, B. (2006). Probabilistic landslide hazards and risk mapping on Penang Island, Malaysia. Journal of Earth System Science, 115, 661-672.

[26]. Lee, S., & Pradhan, B. (2007). Landslide hazard mapping at Selangor, Malaysia using frequency ratio and logistic regression models. Landslides, 4(1), 33-41.

[27]. Lufafa, A., Tenywa, M. M., Isabirye, M., Majaliwa, M. J. G., & Woomer, P. L. (2003). Prediction of soil erosion in a Lake Victoria basin catchment using a GIS-based Universal Soil Loss model. Agricultural systems, 76(3), 883-894.

[28]. Makaya, N., Dube, T., Seutloali, K., Shoko, C., Mutanga, O., & Masocha, M. (2019). Geospatial assessment of soil erosion vulnerability in the upper uMgeni catchment in KwaZulu Natal, South Africa. Physics and Chemistry of the Earth, Parts A/B/C, 112, 50-57.

[29]. McDonald, M. A., Healey, J. R., & Stevens, P. A. (2002). The effects of secondary forest clearance and subsequent land-use on erosion losses and soil properties in the Blue Mountains of Jamaica. Agriculture, Ecosystems & Environment, 92(1), 1-19.

[30]. Méndez-Toribio, M., Meave, J. A., Zermeño-Hernández, I., & Ibarra-Manríquez, G. (2016). Effects of slope aspect and topographic position on environmental variables, disturbance regime and tree community attributes in a seasonal tropical dry forest. Journal of Vegetation Science, 27(6), 1094-1103.

[31]. Montgomery, D. R. (2007). Soil erosion and agricultural sustainability. Proceedings of the National Academy of Sciences, 104(33), 13268-13272.

[32]. Mosavi, A., Sajedi-Hosseini, F., Choubin, B., Taromideh, F., Rahi, G., & Dineva, A. A. (2020). Susceptibility mapping of soil water erosion using machine learning models. Water, 12(7), 1995.

[33]. Mushtaq, F., & Lala, M. G. N. (2017). Assessment of hydrological response as a function of LULC change and climatic variability in the catchment of the Wular Lake, J&K, using geospatial technique. Environmental Earth Sciences, 76, 1-19.

[34]. Mushtaq, F., Farooq, M., Tirkey, A. S., & Sheikh, B. A. (2023). Analytic Hierarchy Process (AHP) Based Soil Erosion Susceptibility Mapping in Northwestern Himalayas: A Case Study of Central Kashmir Province. Conservation, 3(1), 32-52

[35]. Oh, H. J., & Lee, S. (2011). Integration of ground subsidence hazard maps of abandoned coal mines in Samcheok, Korea. International Journal of Coal Geology, 86(1), 58-72.

[36]. Oldeman, L. R., Hakkeling, R. T. A., Sombroek, W. G., & Batjes, N. (1991). Global assessment of human-induced soil degradation (GLASOD). World map of the status of human-induced soil degradation.

[37]. Pandey, A., Mathur, A., Mishra, S. K., & Mal, B. C. (2009). Soil erosion modeling of a Himalayan watershed using RS and GIS. Environmental Earth Sciences, 59, 399-410.

[38]. Parveen, R., & Kumar, U. (2012). Integrated approach of universal soil loss equation (USLE) and geographical information system (GIS) for soil loss risk assessment in Upper South Koel Basin, Jharkhand.

[39]. Pimentel, D., Harvey, C., Resosudarmo, P., Sinclair, K., Kurz, D., McNair, M., ... & Blair, R. (1995). Environmental and economic costs of soil erosion and conservation benefits. Science, 267(5201), 1117-1123.
[40]. Polidori, L., & El Hage, M. (2020). Digital elevation model quality assessment methods: A critical review. Remote sensing, 12(21), 3522.
[41]. Pradeep, G. S., Krishnan, M. N., & Vijith, H. (2015). Identification of critical soil erosion prone areas and annual average soil loss in an upland agricultural watershed of Western Ghats, using analytical hierarchy process (AHP) and RUSLE techniques. Arabian Journal of Geosciences, 8(6), 3697-3711.
[42]. Prasuhn, V., Liniger, H., Gisler, S., Herweg, K., Candinas, A., & Clément, J. P. (2013). A high-resolution soil erosion risk map of Switzerland as strategic policy support system. Land use policy, 32, 281-291.
[43]. Rather, M. A., Satish Kumar, J., Farooq, M., & Rashid, H. (2017). Assessing the influence of watershed characteristics on soil erosion susceptibility of Jhelum basin in Kashmir Himalayas. Arabian Journal of Geosciences, 10(3), 59.
[44]. Raymo, M. E., & Ruddiman, W. F. (1992). Tectonic forcing of late Cenozoic climate. nature, 359(6391), 117-122.
[45]. Renard, K. G. (1997). Predicting soil erosion by water: a guide to conservation planning with the Revised Universal Soil Loss Equation (RUSLE). US Department of Agriculture, Agricultural Research Service.
[46]. Saha, S. (2018). Geo-Environmental Evaluation for Exploring Potential Soil Erosion Areas of Jainti River Basin Using AHP Model, Eastern India. Universal Journal of Environmental Research & Technology, 7(1).
[47]. Saini, S. S., Jangra, R., & Kaushik, S. P. (2015). Vulnerability assessment of soil erosion using geospatial techniques-A pilot study of upper catchment of Markanda river. International journal of advancement in remote sensing, gis and geography, 3(1), 9-21.
[48]. Singh, G. (1981). Soil loss prediction research in India.
[49]. Singh, G., Babu, R., Narain, P., Bhushan, L. S., & Abrol, I. P. (1992). Soil erosion rates in India. Journal of Soil and water Conservation, 47(1), 97-99.
[50]. Tehrany, M. S., Shabani, F., Javier, D. N., & Kumar, L. (2017). Soil erosion susceptibility mapping for current and 2100 climate conditions using evidential belief function and frequency ratio. Geomatics, Natural Hazards and Risk, 8(2), 1695-1714.
[51]. Tiwari, A. K., Risse, L. M., & Nearing, M. A. (2000). Evaluation of WEPP and its comparison with USLE and RUSLE. Transactions of the ASAE, 43(5), 1129-1135.
[52]. Williams, J. R. (1975). Sediment routing for agricultural watersheds 1. JAWRA Journal of the American Water Resources Association, 11(5), 965-974.
[53]. Wu, Q., & Wang, M. (2007). A framework for risk assessment on soil erosion by water using an integrated and systematic approach. Journal of Hydrology, 337(1-2), 11-21.
[54]. Yang, T., Siddique, K. H., & Liu, K. (2020). Cropping systems in agriculture and their impact on soil health-A review. Global Ecology and Conservation, 23, e01118.